INTERNATIONAL SOCIETY FOR SOIL MECHANICS AND GEOTECHNICAL ENGINEERING



This paper was downloaded from the Online Library of the International Society for Soil Mechanics and Geotechnical Engineering (ISSMGE). The library is available here:

https://www.issmge.org/publications/online-library

This is an open-access database that archives thousands of papers published under the Auspices of the ISSMGE and maintained by the Innovation and Development Committee of ISSMGE.

The paper was published in the proceedings of the 11th International Conference on Scour and Erosion and was edited by Thor Ugelvig Petersen and Shinji Sassa. The conference was held in Copenhagen, Denmark from September 17th to September 21st 2023.

An Eulerian two-phase model investigation on wave-induced scour around a vertical circular cylinder

Benjamin Tsai^{1*}, Antoine Mathieu¹, Tian-Jian Hsu¹, and Julien Chauchat²

ABSTRACT

A three-dimensional Eulerian two-phase flow solver, SedFoam, has been developed for various sediment transport applications. The solver has demonstrated success in modeling sheet flow and bedforms driven by oscillatory flows using a Reynolds-averaged Navier–Stokes (RANS) formulation. However, the accuracy of the RANS formulation for more complex flows, such as scour around structures, requires further evaluation. SedFoam has recently been enhanced to incorporate two-phase large-eddy simulation (LES) capability. In this study, RANS and LES approaches are tested via a three-dimensional case of wave-induced local scour around a single vertical circular pile. Two laboratory experiments, one with an erodible bed and the other with a rigid bed, were chosen for simulation, with both experiments having a Keulegan-Carpenter (KC) number of 10. The $k-\omega$ turbulence closure was selected for the RANS simulation, and the dynamic Lagrangian subgrid closure was chosen for the LES simulation. Numerical results reveal that both RANS and LES simulations can resolve lee-wake vortices, although the vortices are significantly weaker in the RANS simulation. In comparison with the LES results, the RANS approach fails to predict horseshoe vortex with sufficient intensity, leading to an underestimation of scour hole depth development. Although the scour depths develop at a very similar rate in the early stage, the scour depth predicted by the RANS simulation quickly reaches equilibrium, while the LES simulation follows the measured trend. These findings indicate that a turbulence-resolving methodology, i.e. LES, is necessary for accurate scour simulations.

INTRODUCTION

Conventional scour models typically assume sediment transport processes can be separated into bedload and suspended load, requiring, for instance, an empirical pickup function to initiate sediment suspension. To reduce the number of assumptions, the Eulerian-Eulerian two-phase approach has been developed, which solves both sediment and fluid phase mass and momentum conservation as continua. The two phases interact with each other based on fundamental physical laws and incorporate particle stress closure to model intergranular interactions across a wide range of sediment concentrations. Consequently, the full dynamics of transport, including soil strength and seepage flow, can be modeled within a holistic system. In this study, we adopt an open-source Eulerian two-phase model, SedFoam (https://github.com/sedFoam) (Cheng et al. 2017;

¹ Center for Applied Coastal Research, University of Delaware, Newark, DE 19716, USA.

² LEGI, University of Grenoble Alpes, G-INP, CNRS, 38000 Grenoble, France.

^{*} Corresponding author; e-mail: <u>btsai@udel.edu</u>

Chauchat et al. 2017), developed using the OpenFOAM Computational Fluid Dynamics (CFD) toolbox, to investigate scour around a circular pile driven by oscillatory flow.

SedFoam, which solves RANS equations with a two-equation closure, has been demonstrated over the past several years to be capable of simulating current and wave-driven sheet flow transport (Cheng et al. 2017; Kim et al. 2018, 2019) as well as wave-driven bedform evolutions (Salimi-Tarazouj et al. 2021). Its capability has also been shown in simulating scour below a two-dimensional pipeline (Mathieu et al. 2019; Tsai et al. 2022) and three-dimensional scour around a vertical cylinder (Nagel et al. 2020) driven by steady flow. While the RANS approach has been widely used to model flow around structures and can generally capture key flow features around a vertical cylinder, it is well-known to struggle with predicting the horseshoe vortex in front of the cylinder and tends to predict weaker lee-wake vortices due to high diffusivity (Lai et al. 2022). As a result, a turbulence-resolved approach, such as LES, is needed, and SedFoam has recently been expanded to include LES capability to better resolve sheet flow processes (Cheng et al. 2018; Mathieu et al. 2021, 2022).

The objective of this study is to employ SedFoam as a tool to examine the significance of resolving turbulent coherent structures in scour modeling. This is achieved by simulating laboratory experiments reported by Sumer et al. (1997, 2013) that investigate turbulent flow and scour depth around a vertical cylinder driven by waves.

METHOD

Model Formulations

SedFoam solves mass and momentum conservation equations for both fluid and sediment phases, which can be expressed as follows:

$$\frac{\partial (1-\alpha)}{\partial t} + \frac{\partial (1-\alpha)u_i^f}{\partial x_i} = 0 \tag{1}$$

$$\frac{\partial \alpha}{\partial t} + \frac{\partial \alpha u_i^s}{\partial x_i} = 0 \tag{2}$$

$$\frac{\partial \rho^{f} (1-\alpha) u_{i}^{f}}{\partial t} + \frac{\partial \rho^{f} (1-\alpha) u_{i}^{f} u_{j}^{f}}{\partial x_{i}} = -\frac{\partial p^{f}}{\partial x_{i}} + \frac{\partial \tau_{ij}^{f}}{\partial x_{j}} + \rho^{f} (1-\alpha) g_{i} + (1-\alpha) f_{i} - M_{i}$$
(3)

$$\frac{\partial \rho^s \alpha u_i^s}{\partial t} + \frac{\partial \rho^s \alpha u_i^s u_j^s}{\partial x_i} = -\frac{\partial p^s}{\partial x_i} + \frac{\partial \tau_{ij}^s}{\partial x_j} + \rho^s \alpha g_i + \alpha f_i + M_i$$
(4)

In this study, the superscripts f and s denote the fluid and sediment phases, respectively, while the subscript i = 1, 2, 3 represents the x, y, z components, respectively. All the following quantities are either Favre-averaged (for RANS approach) or Favre-filtered (for LES approach), but the system of equations is equivalent for both methodologies. α represents the sediment volumetric concentration, ρ denotes density, g is the gravity, and u is the velocity. p and τ represent the normal stress (pressure) and the deviatoric stress (shear stress), respectively. An external pressure gradient, f_i , is used to drive the flow. The inter-phase momentum coupling term, M_i , represents the drag force and pressure gradient force coupling the two phases, which is expressed as:

$$M_{i} = -\alpha \frac{\partial p^{f}}{\partial x_{i}} + \alpha K \left(u_{i}^{f} - u_{i}^{s} \right) - \Gamma_{i}$$
(5)

where K is the drag parameter, v_t is the turbulent viscosity, and σ_c is the Schmidt number. The first term on the right-hand side represents the buoyancy force. The following two terms are due to drag force. The second term represents the drag induced by velocity difference between fluid and sediment phase. The third term, Γ results from unresolved correlations between fluid velocity and sediment concentration fluctuations. In RANS, it cannot be neglected and is modeled using a gradient-diffusion model. However, in LES, Γ can be neglected when the grid size is on the order of the particle diameter (Ozel et al. 2013). It can be shown as follow:

$$\Gamma_{i} = \begin{cases} K \frac{v_{t}^{f}}{\sigma_{c}} \frac{\partial \alpha}{\partial x_{i}} &, \text{ for RANS} \\ 0 &, \text{ for LES} \end{cases}$$
(6)

in which v_t is the turbulent viscosity and σ_c is the Schmidt number. Several options of K are available in SedFoam, we adopt Ding and Gidaspow (1990) formulation which is written as

$$K = \begin{cases} \frac{150\alpha v^{f} \rho^{f}}{(1-\alpha)d^{2}} + \frac{1.75\rho^{f} \left| u_{i}^{f} - u_{i}^{s} \right|}{d} , \alpha \geq 0.2\\ \frac{3}{4} C_{D} \frac{\rho^{f} \left| u_{i}^{f} - u_{i}^{s} \right|}{d} (1-\alpha)^{-1.65} , \alpha < 0.2 \end{cases}$$
(7)

in which v is the viscosity, d denotes the median particle diameter, and C_D denotes the drag coefficient.

Pressure and shear stress of the sediment phase are modeled by a collisional component (super-script 'sc') in the low to intermediate concentration regime, and a frictional component (super-script 'sf') for high concentration regime of enduring contact,

$$p^s = p^{sc} + p^{sf} \tag{8}$$

$$\tau_{ij}^s = \tau_{ij}^{sc} + \tau_{ij}^{sf} \tag{9}$$

The kinetic theory of granular flow takes over the collisional component and models by the granular temperature. To avoid overcrowd with this paper, readers may refer to Chauchat et al. (2017) and Mathieu et al. (2022) for more detailed description on the kinetic theory of granular flow. An empirical formula for the frictional component of sediment pressure is provided by Johnson and Jackson (1987) which is written as

$$p^{sf} = \begin{cases} 0 & , & \alpha < 0.57 \\ 0.05 \frac{(\alpha - 0.57)^3}{(0.635 - \alpha)^5} & , & \alpha \ge 0.57 \end{cases}$$
 (10)

Following Srivastava and Sundaresan (2003), the shear stress τ_{ij}^{s} is calculated by

$$\tau_{ij}^{s} = \frac{p^{sf} \sin \theta_{f}}{\sqrt{2S_{ij}^{s}S_{ij}^{s} + D_{small}^{2}}} S_{ij}^{s}$$
(11)

in which θ_f is the friction angle set to be 32°, S_{ij} is the shear strain rate tensor, and D_{small} is a very small nominal strain rate which serves numerically to avoid dividing by zero.

In this study, two turbulent modeling approaches (i.e., RANS and LES) are being tested. RANS models turbulence as a diffusion process and can be described by the turbulent viscosity v_t , the formulation is shown as

$$\tau_{ij}^{f} = \rho^{f} \left(1 - \alpha \right) \left[2 \left(v^{f} + v_{t}^{f} \right) S_{ij}^{f} - \frac{2}{3} \frac{\partial u_{k}^{f}}{\partial x_{k}} \delta_{ij} \right]$$

$$(12)$$

Two-equation turbulence closure models are mostly used. A two-phase k- ω model (Chauchat et al. 2017) is adopted in this study which is shown as

$$v_{t}^{f} = \frac{k}{\max \left[\omega, C_{\lim} \frac{\left\| S_{ij}^{f} \right\|}{\sqrt{C_{u}}} \right]}$$
(13)

where C_{lim} is a stress limiter coefficient, k is the turbulent kinetic energy, and ω is the specific turbulent energy dissipation rate. k and ω are calculated by their balance equations:

$$\frac{\partial k}{\partial t} + u_j^f \frac{\partial k}{\partial x_j} = R_{ij}^f \frac{\partial u_i^f}{\partial x_j} + \frac{\partial}{\partial x_j} \left[\left(v^f + \frac{v_t^f}{\sigma_k} \right) \frac{\partial k}{\partial x_j} \right] - C_\mu \omega k - \frac{2K \left(1 - t_{mf} \right) \alpha k}{\rho^f} - \frac{1}{1 - \alpha} \frac{v_t^f}{\sigma_k} \frac{\partial \alpha}{\partial x_j} \left(\frac{\rho^s}{\rho^f} - 1 \right) g_j \tag{14}$$

and

$$\frac{\partial \omega}{\partial t} + u_{j}^{f} \frac{\partial \omega}{\partial x_{j}} = C_{1\omega} \frac{\omega}{k} R_{ij}^{f} \frac{\partial u_{i}^{f}}{\partial x_{j}} + \frac{\partial}{\partial x_{j}} \left[\left(v^{f} + \frac{v_{t}^{f}}{\sigma_{\omega}} \right) \frac{\partial \omega}{\partial x_{j}} \right]
- C_{2\omega} \omega^{2} - C_{3\omega} \frac{2K \left(1 - t_{mf} \right) \alpha \omega}{\rho^{f}} - \frac{C_{4\omega}}{1 - \alpha} \frac{\omega}{k} \frac{v_{t}^{f}}{\sigma_{c}} \frac{\partial \alpha}{\partial x_{j}} \left(\frac{\rho^{s}}{\rho^{f}} - 1 \right) g_{j} + \sigma_{d} \frac{1}{\omega} \frac{\partial k}{\partial x_{j}} \frac{\partial \omega}{\partial x_{j}} \tag{15}$$

Multiple model coefficients are used in the above k and ω equations, readers may refer to Chauchat et al. (2017) for more details. Different than RANS, LES resolves turbulence that larger than a certain filtering length (usually the grid size). The formulation is shown as follow,

$$\tau_{ij}^{f} = \rho^{f} \left(1 - \alpha \right) \left(2 v^{f} S_{ij}^{f} - \frac{2}{3} \frac{\partial u_{k}^{f}}{\partial x_{k}} \delta_{ij} \right) + \tau_{ij}^{f,sgs}$$

$$(16)$$

Any turbulent motion smaller than the filtering length (subgrid scale, sgs) will be modeled by a chosen subgrid closure. The dynamic Lagrangian subgrid closure model (Meneveau et al. 1996) is used in this study which can be written as

$$\tau_{ij}^{s,sgs} = \rho^f (1 - \alpha) \Delta^2 |S_{ij}^f| \left(2C_1^f S_{ij}^f - \frac{2}{3} C_2^f S_{kk}^f \right)$$
 (17)

where Δ is the grid size, C_1 and C_2 are model coefficients. Readers are suggested to refer to Mathieu et al. (2022) for more detailed description of the LES subgrid closure.

Physical Experiments

Two sets of physical experiments are utilized in this study to validate the RANS and LES models. The first dataset is a rigid bed experiment with a vertical cylinder conducted by Sumer et al. (1997). This experiment was carried out in a wave flume with dimensions of 0.8 m in depth, 0.6 m in width, and 26.5 m in length. The water depth was set at 0.4 m, and regular waves were generated using a piston-type wave maker. Free-stream velocity and bed shear stress were measured. Flow structures were visualized using the hydrogen-bubble technique around the cylinder near the bed. One of the experiments featuring a vertical pile with a diameter of 40 mm is selected, with a wave period of 4.4 s and a wave orbital velocity amplitude of 9.4 cm/s, resulting in a *KC* number of 10.3 (Table 1).

The second dataset is an erodible bed experiment reported by Sumer et al. (2013), who investigated scour under steady current and/or waves around a circular pile of the same diameter (see Table 1). Irregular waves were used in the experiments with a peak wave period of 1.79 s and a maximum orbital velocity amplitude of 22.5 cm/s. The resulting KC number is 10.1, which is very close to that in the rigid bed experiment. The sediment consisted of fine sand with a median diameter of 0.17 mm. The measured non-dimensional equilibrium scour depth (S_{eq}/D) is 0.28, and the time scale of the scour process (T) is 90 s, as reported by Sumer et al. (2013). The development of the scour depth towards equilibrium can be described by an empirical formula (Sumer et al. 1993), written as:

$$\frac{S}{D} = \frac{S_{eq}}{D} \left(1 - e^{-\frac{t}{T}} \right) \tag{18}$$

This will later be compared with the model results.

Table 1. Wave conditions of physical experiments used in this study.

Bed type	Pile diameter, D [cm]	Wave period, $T_w[s]$	Maximum flow velocity, U_m [cm/s]	Keulegan-Carpenter number, <i>KC</i> [-]
Rigid bed	4	4.4	9.4	10.3
Erodible bed	4	1.79	22.5	10.1

Model Domain

A total of four simulations are conducted to investigate the differences between the RANS and LES approaches for simulating wave-driven scour for both rigid and erodible beds under similar flow conditions. The numerical domain measures 0.4 m in width, 0.6 m in length, and 0.2 m in height, with a circular cylinder of 4 cm diameter located at the center. Cyclic boundary conditions are employed for the inlet, outlet, and side patches, while wall boundary conditions are applied to the cylinder surface and the bottom of the domain. The top boundary utilizes a zero-gradient boundary condition. A stretching mesh is employed for this study, providing a finer grid around the cylinder, with the grid size gradually increasing as it moves away from the cylinder. The finest grid size for the RANS model domain measures 0.51 mm by 0.51 mm by 0.34 mm in the streamwise, spanwise, and vertical directions, respectively. For the LES model, a slightly higher

resolution is used, with the finest grid size being a 0.3 mm cube to ensure that the first grid point from the wall boundary remains smaller than five wall units for most of the simulation time. The total number of mesh cells amount to three and nine million for the RANS and LES domains, respectively. The time step is controlled by the Courant–Friedrichs–Lewy condition with a value of 0.1.

RESULTS

Erodible Bed

The temporal evolution of scour hole depth development, as predicted by the RANS and LES models, along with the empirical fit to the measured data, is shown in Figure 1. The RANS model reaches the equilibrium scour depth in approximately ten waves, which is significantly faster than the experimental fitting curve (i.e. Equation (18)). Moreover, the RANS model predicts an equilibrium scour depth of approximately 0.05D, substantially underestimating the measured value of 0.28D. Conversely, the LES results, up to about t=70 sec (due to higher computational costs, this is the most updated simulation result available at the moment), show significantly better agreement with the measured data. The LES model has the potential to reach the final equilibrium scour depth, with simulations currently in progress.

Compared to the underestimation of the scour hole depth in this study, the single-phase RANS model by Baykal et al. (2017) exhibits overestimation. Among several differences between the two models, such as the absence of the M_i term in the single-phase model and different sediment transport modeling approaches, the key factor that causes the underestimation in this study is found to be the k- ω formulations. In addition to the extra turbulence damping terms included in the two-phase k- ω formulations, the Pope's correction (Pope 1978; Wilcox 2008) was not incorporated in this study. Instead, a constant $C_{2\omega}$ is used, implying no vortex stretching (Pope 1978; Wilcox 2008). The aforementioned reasons may explain the difference between the single-phase RANS model by Baykal et al. (2017) and this study (two-phase model). However, further investigation is necessary to clarify the discrepancy.

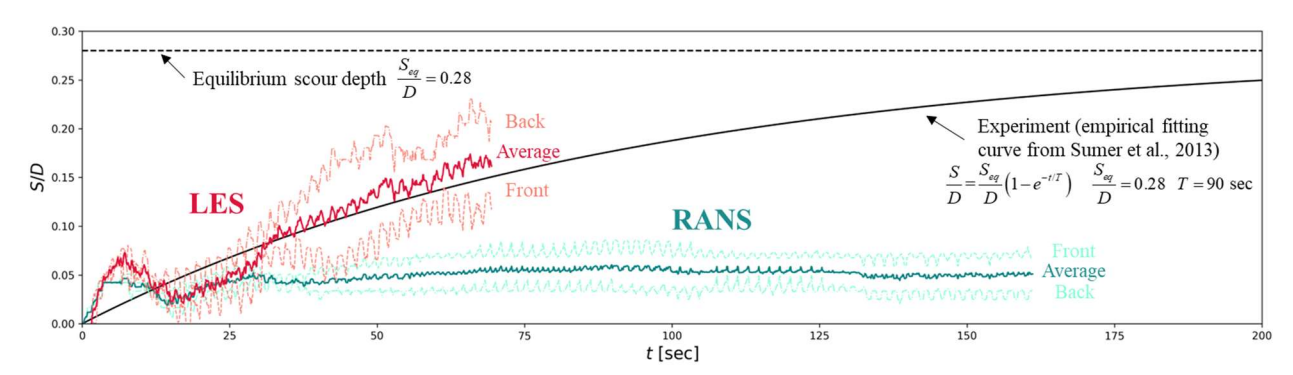


Figure 1. Scour depth development of RANS and LES.

Two types of flow features, namely horseshoe and lee-wake vortices, largely contribute to local scour (Lai et al. 2022). The *Q*-criterion (Hunt et al. 1988) is employed to identify vortices,

which are based on the local velocity gradient tensor. LES approach resolves more intense turbulent coherent structures generated around the cylinder, whereas RANS approach is more diffusive, and the resolved coherent structures are much weaker (Figure 2). Although both RANS and LES models are capable of predicting lee-wake vortices, LES results exhibit larger turbulent intensity, as the intensity of the contour is set to Q = 4000, compared to Q = 1000 for RANS results. Additionally, the RANS model predicts more homogeneous lee-wake vortices, while LES model resolves much more irregular turbulent features. Lastly, RANS model predicts virtually no horseshoe vortex, whereas they can be clearly seen in LES results. These stronger vortices predicted by LES model result in a deeper scour depth (Figure 3b). The key difference between RANS and LES, namely the prediction of the horseshoe vortex, directly contributes to the scour hole development. The stronger horseshoe vortex predicted by LES leads to increased sediment entrainment and transport, consequently forming a deeper scour hole.

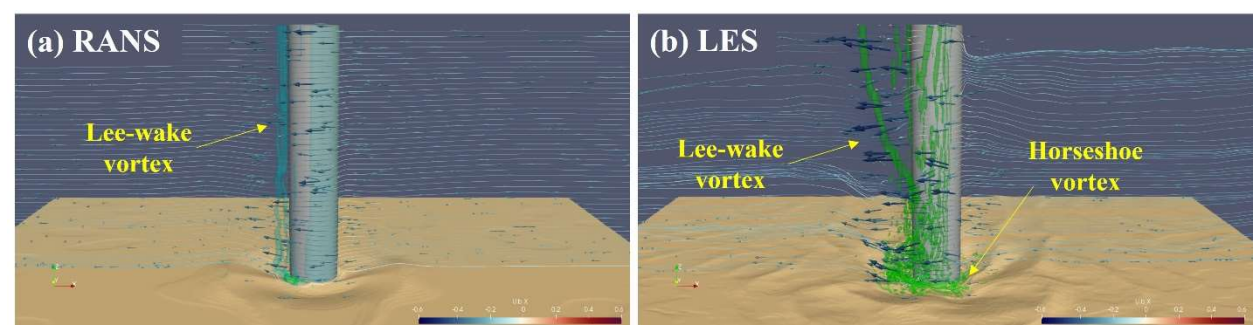


Figure 2. Snapshots of the sediment bed and turbulent coherent structure at t = 60.3 sec using (a) RANS and (b) LES. The cyan and green iso-surfaces denote the Q criterion using Q = 1000 and 4000, respectively. The arrows and streamlines show the flow direction.

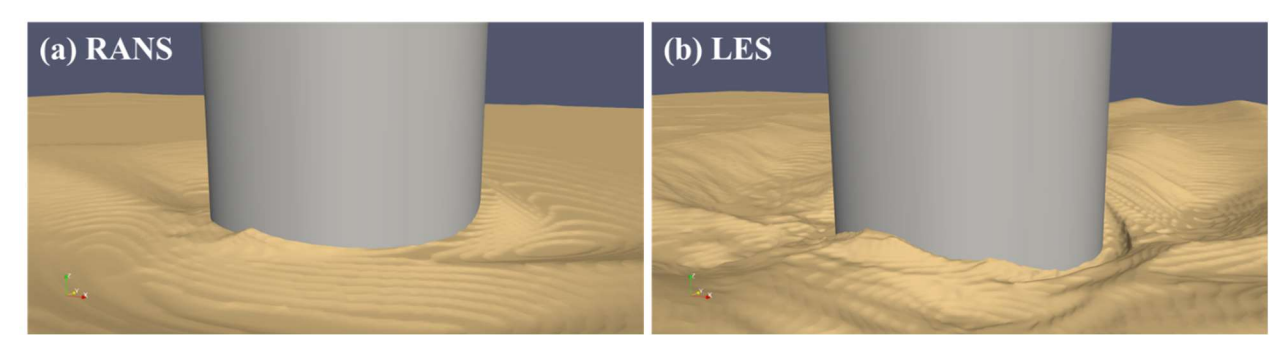


Figure 3. Close-up view of the scour hole of (a) RANS and (b) LES results.

Rigid Bed

Sumer et al. (1997) observed vortex shedding during the experiment They demonstrated that attached vortices are washed around the cylinder during flow reversal, followed by a shed vortex behind it. The rigid bed results also indicate that the LES approach is capable of capturing the expected turbulent coherent structures (Figure 4). Meanwhile, the model results reveal that the

RANS model underpredicts the bed shear stress, which is consistent with the results from the single-phase model (Baykal et al. 2017).

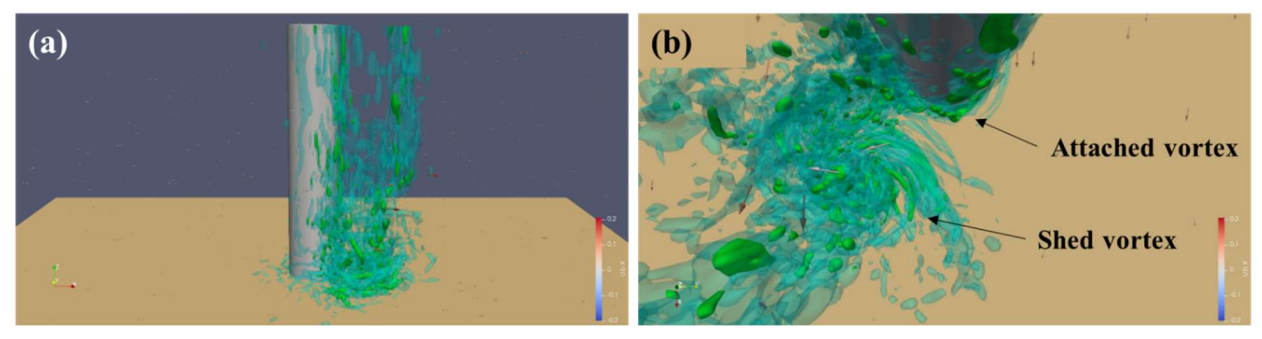


Figure 4. The turbulent coherent structures resolved by LES visualized using the Q-method with Q = 500 (cyan) and 1500 (green) during flow reversal.

CONCLUSION

The Eulerian two-phase model, SedFoam, has been applied to study three-dimensional wave-induced local scour around a single vertical circular pile. Experiments with a Keulegan-Carpenter (KC) number of 10 are chosen to be simulated and RANS and LES results are compared. The numerical results show that both RANS and LES approaches can resolve the lee-wake vortices, yet RANS model predicts much weaker vortices. Compared with LES approach, RANS approach also fails to predict the horseshoe vortex. Similar results are shown in the rigid bed case. This leads to an underestimation of scour hole development, and the RANS simulation quickly reaches the equilibrium scour depth, whereas LES simulation follows the experimental trend very well. The results indicate that a turbulence-resolving model, i.e. LES, is necessary for simulating scour around structures.

ACKNOWLEDGEMENT

This study is supported by U.S. Strategic Environmental Research and Development Program (MR20-1478) and National Science Foundation (CMMI-2050854). Numerical simulations presented in this study were carried out using the Caviness and Darwin clusters at University of Delaware and Expanse cluster at SDSC via ACCESS.

REFERENCES

- Baykal, C., B. M. Sumer, D. R. Fuhrman, N. G. Jacobsen, and J. Fredsøe. 2017. "Numerical simulation of scour and backfilling processes around a circular pile in waves." *Coast. Eng.*, 122: 87–107. https://doi.org/10.1016/j.coastaleng.2017.01.004.
- Chauchat, J., Z. Cheng, T. Nagel, C. Bonamy, and T.-J. Hsu. 2017. "SedFoam-2.0: a 3-D two-phase flow numerical model for sediment transport." *Geosci. Model Dev.*, 10 (12): 4367–4392. https://doi.org/10.5194/gmd-10-4367-2017.
- Cheng, Z., T.-J. Hsu, and J. Calantoni. 2017. "SedFoam: A multi-dimensional Eulerian two-phase model for sediment transport and its application to momentary bed failure." *Coast. Eng.*, 119: 32–50. https://doi.org/10.1016/j.coastaleng.2016.08.007.
- Cheng, Z., T.-J. Hsu, and J. Chauchat. 2018. "An Eulerian two-phase model for steady sheet flow using large-eddy simulation methodology." *Adv. Water Resour.*, 111: 205–223. https://doi.org/10.1016/j.advwatres.2017.11.016.
- Ding, J., and D. Gidaspow. 1990. "A bubbling fluidization model using kinetic theory of granular flow." *AIChE J.*, 36 (4): 523–538. John Wiley & Sons, Ltd. https://doi.org/10.1002/aic.690360404.
- Hunt, J. C. R., A. A. Wray, and P. Moin. 1988. "Eddies, streams, and convergence zones in turbulent flows." *Cent. Turbul. Res. Proc. Summer Program 1988*, 193–208.
- Johnson, P. C., and R. Jackson. 1987. "Frictional-collisional constitutive relations for granular materials, with application to plane shearing." *J. Fluid Mech.*, 176: 67–93. https://doi.org/10.1017/S0022112087000570.
- Kim, Y., Z. Cheng, T.-J. Hsu, and J. Chauchat. 2018. "A Numerical Study of Sheet Flow Under Monochromatic Nonbreaking Waves Using a Free Surface Resolving Eulerian Two-Phase Flow Model." *J. Geophys. Res. Oceans*, 123 (7): 4693–4719. https://doi.org/10.1029/2018JC013930.
- Kim, Y., R. S. Mieras, Z. Cheng, D. Anderson, T.-J. Hsu, J. A. Puleo, and D. Cox. 2019. "A numerical study of sheet flow driven by velocity and acceleration skewed near-breaking waves on a sandbar using SedWaveFoam." *Coast. Eng.*, 152: 103526. https://doi.org/10.1016/j.coastaleng.2019.103526.
- Lai, Y. G., X. Liu, F. A. Bombardelli, and Y. Song. 2022. "Three-Dimensional Numerical Modeling of Local Scour: A State-of-the-Art Review and Perspective." *J. Hydraul. Eng.*, 148 (11): 03122002. American Society of Civil Engineers. https://doi.org/10.1061/(ASCE)HY.1943-7900.0002019.
- Mathieu, A., J. Chauchat, C. Bonamy, G. Balarac, and T.-J. Hsu. 2021. "A finite-size correction model for two-fluid large-eddy simulation of particle-laden boundary layer flow." *J. Fluid Mech.*, 913. https://doi.org/10.1017/jfm.2021.4.
- Mathieu, A., J. Chauchat, C. Bonamy, and T. Nagel. 2019. "Two-Phase Flow Simulation of Tunnel and Lee-Wake Erosion of Scour below a Submarine Pipeline." *Water*, 11 (8): 1727. https://doi.org/10.3390/w11081727.

- Mathieu, A., Z. Cheng, J. Chauchat, C. Bonamy, and T.-J. Hsu. 2022. "Numerical investigation of unsteady effects in oscillatory sheet flows." *J. Fluid Mech.*, 943: A7. Cambridge University Press. https://doi.org/10.1017/jfm.2022.405.
- Meneveau, C., T. S. Lund, and W. H. Cabot. 1996. "A Lagrangian dynamic subgrid-scale model of turbulence." *J. Fluid Mech.*, 319: 353–385. Cambridge University Press. https://doi.org/10.1017/S0022112096007379.
- Nagel, T., J. Chauchat, C. Bonamy, X. Liu, Z. Cheng, and T.-J. Hsu. 2020. "Three-dimensional scour simulations with a two-phase flow model." *Adv. Water Resour.*, 138: 103544. https://doi.org/10.1016/j.advwatres.2020.103544.
- Ozel, A., P. Fede, and O. Simonin. 2013. "Development of filtered Euler–Euler two-phase model for circulating fluidised bed: High resolution simulation, formulation and a priori analyses." *Int. J. Multiph. Flow*, 55: 43–63. https://doi.org/10.1016/j.ijmultiphaseflow.2013.04.002.
- Pope, S. B. 1978. "An explanation of the turbulent round-jet/plane-jet anomaly." *AIAA J.*, 16 (3): 279–281. American Institute of Aeronautics and Astronautics. https://doi.org/10.2514/3.7521.
- Salimi-Tarazouj, A., T.-J. Hsu, P. Traykovski, Z. Cheng, and J. Chauchat. 2021. "A Numerical Study of Onshore Ripple Migration Using a Eulerian Two-phase Model." *J. Geophys. Res. Oceans*, 126 (2): e2020JC016773. https://doi.org/10.1029/2020JC016773.
- Srivastava, A., and S. Sundaresan. 2003. "Analysis of a frictional–kinetic model for gas–particle flow." *Powder Technol.*, 129 (1): 72–85. https://doi.org/10.1016/S0032-5910(02)00132-8.
- Sumer, B. M., N. Christiansen, and J. Fredsøe. 1993. "Influence of Cross Section on Wave Scour around Piles." *J. Waterw. Port Coast. Ocean Eng.*, 119 (5): 477–495. American Society of Civil Engineers. https://doi.org/10.1061/(ASCE)0733-950X(1993)119:5(477).
- Sumer, B. M., N. Christiansen, and J. Fredsøe. 1997. "The horseshoe vortex and vortex shedding around a vertical wall-mounted cylinder exposed to waves." *J. Fluid Mech.*, 332: 41–70. https://doi.org/10.1017/S0022112096003898.
- Sumer, B. M., T. U. Petersen, L. Locatelli, J. Fredsøe, R. E. Musumeci, and E. Foti. 2013. "Backfilling of a Scour Hole around a Pile in Waves and Current." *J. Waterw. Port Coast. Ocean Eng.*, 139 (1): 9–23. https://doi.org/10.1061/(ASCE)WW.1943-5460.0000161.
- Tsai, B., A. Mathieu, E. P. Montellà, T.-J. Hsu, and J. Chauchat. 2022. "An Eulerian two-phase flow model investigation on scour onset and backfill of a 2D pipeline." *Eur. J. Mech. BFluids*, 91: 10–26. https://doi.org/10.1016/j.euromechflu.2021.09.004.
- Wilcox, D. C. 2008. "Formulation of the k-w Turbulence Model Revisited." *AIAA J.*, 46 (11): 2823–2838. https://doi.org/10.2514/1.36541.